

Lattice dynamics for isochorically heated metals: A model study

Shota Ono*

Department of Electrical, Electronic and Computer Engineering, Gifu University, Gifu 501-1193, Japan

The electron-excitation induced bond strength variations in metals have been predicted from density-functional theory calculations and observed experimentally, while the microscopic mechanism has yet to be elucidated. Here, we present a minimal model that reproduces the phonon hardening and softening for fcc- and bcc-structured metals as a result of the electron thermal excitation. We explain why the phonon mode softens at the N point for bcc-structured metals.

I. INTRODUCTION

The effect of strong nonequilibrium condition between electrons and phonons on solid state properties has been investigated both experimentally and theoretically. It influences not only thermodynamic properties, such as the electron specific heat and density-of-states [1], but also the lattice dynamics spectra (i.e., phonon dispersion relations). Since the values of the force constants for ions are determined by the adiabatic potential that is a sum of the ion-ion repulsive and the ion-electron-ion interaction potential energies, it is possible to manipulate the lattice dynamics spectra by tuning the electron-mediated interaction potential. Based on density-functional theory (DFT) calculations, Recoules *et al.* have predicted that the phonon frequencies of Au increase over the entire Brillouin zone (BZ) when the electron temperature T_e is increased up to several eV [2]. This is understood as a decrease in the electron-ion screening as a result of the thermal excitation of $5d$ -electrons located below the Fermi level by a few eV. The femtosecond pump-probe technique has confirmed the bond hardening as an increase in the melting temperature of Au [3], which paves the way for understanding the fundamental properties of warm-dense aluminum [4], copper [5], molybdenum [6], and electron gas [7].

By this argument recent studies based on DFT calculations in Ref. [8–11] is interesting; Even if d -electrons are absent in a system, a noticeable change in the phonon dispersion relations has been predicted when T_e increases. For example, fcc-structured metals such as Al show a phonon hardening over the entire BZ, while bcc-structured metals such as Na show a phonon softening at the point N within the BZ [9]. A similar conclusion has been reached in a recent study [10], where the neutral pseudoatom model developed from DFT and molecular dynamics simulations has been used. Interestingly, Bottin *et al.* have shown that for both Al and Au crystals the monovacancy formation enthalpy increases with T_e (i.e., the bond hardening), while its origin is different: The largest contribution to the stress is from the kinetic energy part for Al and the pseudopotential (ion-electron potential) energy part for Au [11]. Since Al and Na are

a typical free-electron metal in the ground state, as well as the supporting evidence for high T_e [11], it must be possible to develop a simple model to understand such a crystal structure dependence of the phonon property.

In this paper, we construct a minimal model for phonons in isochorically heated nearly free-electron metals and calculate the T_e -dependence of the phonon dispersion relations. The phonon hardening and softening occur in fcc- and bcc-structured metals, respectively, which are consistent with DFT based calculations [9, 10]. The phonon hardening originates from a significant increase in the force constant for the first nearest neighbor (NN) sites, while the phonon softening at the N point in bcc-structured metals originates from a delicate balance between force constants for the first and second NN sites.

II. FORMULATION

To compute the phonon dispersion relations in metals, we extend the theory of the lattice dynamics for simple metals at $T_e = 0$ K [12] to the case at $T_e \neq 0$ K. We consider a simple metal that consists of ions and conducting electrons. Each ion and electron have charges Ze and $-e$, respectively, where Z is the valence of the ion. With a charge neutrality condition, the number of electrons is uniquely determined when that of ions is given. We assume that the total potential energy between ions separated by a distance R is

$$V_{\text{tot}}(R) = v_{\text{d}}(R) + v_{\text{ind}}(R), \quad (1)$$

where v_{d} is the direct interaction potential between ions and given by

$$v_{\text{d}}(R) = \frac{Z^2 e^2}{4\pi\epsilon_0 R} \quad (2)$$

with the dielectric constant of vacuum ϵ_0 . v_{ind} in Eq. (1) is the indirect interaction potential that is derived from the electron-mediated ion-ion interaction. This is written as (see Appendix A for the derivation)

$$v_{\text{ind}}(R) = \int_0^\infty dq C(q) \frac{\sin(qR)}{qR} \quad (3)$$

with the wavenumber q . The kernel $C(q)$ in Eq. (3) is

$$C(q) = - \left(\frac{\epsilon_0 q^4}{2\pi^2 e^2} \right) v_{\text{ps}}^2(q) \frac{\chi(q, T_e)}{1 + [1 - G(q)]\chi(q, T_e)}, \quad (4)$$

*Electronic address: shota_o@gifu-u.ac.jp

where $v_{\text{ps}}(q)$ is the Fourier component of the model pseudopotential. $\chi(q, T_e)$ is the T_e -dependent response function and explicitly written as

$$\chi(q, T_e) = \frac{4}{\pi k_{\text{F}} a_{\text{B}} y^2} \int_0^\infty dx \frac{x}{y} f(x, T_e) \ln \left| \frac{2 + y/x}{2 - y/x} \right| \quad (5)$$

with the Fermi wavenumber k_{F} , the Bohr radius a_{B} , $x = k/k_{\text{F}}$, $y = q/k_{\text{F}}$, and the Fermi-Dirac distribution function

$$f(x, T_e) = \left[e^{(\varepsilon_{\text{F}} x^2 - \mu)/(k_{\text{B}} T_e)} \right]^{-1} \quad (6)$$

with the Fermi energy ε_{F} at $T_e = 0$ K, the chemical potential μ , and the Boltzmann constant k_{B} . When $T_e = 0$ K, Eq. (5) can be reduced to the Hartree formula [12]

$$\chi(q, 0) = \frac{4}{\pi k_{\text{F}} a_{\text{B}} y^2} \left(\frac{1}{2} + \frac{4 - y^2}{8y} \ln \left| \frac{2 + y}{2 - y} \right| \right). \quad (7)$$

In our model, the effect of T_e (i.e., electron occupation) on the phonon dispersion relations is entered into $\chi(q, T_e)$. Finally, $G(q)$ in Eq. (4) accounts for the effects of exchange and correlation. The model functions $v_{\text{ps}}(q)$ and $G(q)$ with material parameters will be given later.

The phonon dispersion relations for the central potential of Eq. (1) are calculated by a diagonalization of the dynamical matrix [13]

$$\mathcal{D}(\mathbf{q}) = \sum_l \sin^2 \left(\frac{\mathbf{q} \cdot \mathbf{R}_l}{2} \right) \left[\mathbf{A} \mathbf{1} + B \hat{R}_l \hat{R}_l \right], \quad (8)$$

where \mathbf{q} is the wavevector of phonons, $\mathbf{R}_l = (R_{lx}, R_{ly}, R_{lz})$ is the l th ion position, $\mathbf{1}$ is the 3×3 unit matrix, and $\hat{R}_l \hat{R}_l$ is the dyadic formed from the unit vectors $\hat{R}_l = \mathbf{R}_l / |\mathbf{R}_l|$. A and B are the force constants defined as

$$A = \frac{2}{R_l} \left. \frac{dV_{\text{tot}}(R)}{dR} \right|_{R=R_l}, \quad (9)$$

$$B = 2 \left[\left. \frac{d^2 V_{\text{tot}}(R)}{dR^2} \right|_{R=R_l} - \frac{1}{R_l} \left. \frac{dV_{\text{tot}}(R)}{dR} \right|_{R=R_l} \right], \quad (10)$$

where the derivatives of V_{tot} are evaluated at $R_l = |\mathbf{R}_l|$. For later use, we define A_p and B_p as the force constant of Eqs. (9) and (10) for the p th NN ions. The phonon frequencies are given by $\omega = \sqrt{\lambda / M_{\text{ion}}}$ with the ion mass M_{ion} and three eigenvalues λ of Eq. (8).

III. RESULTS AND DISCUSSION

We study the phonon properties of Al ($Z = 3$) and Na ($Z = 1$) that show a fcc and bcc structure in the ground state, respectively. The lattice constant is $a_{\text{lat}} = 4.049$ Å for Al and 4.225 Å for Na. The Wigner-Seitz radius is $r_s = 2.07$ for Al and 3.93 for Na (in units of Bohr radius

a_{B}) [13]. The Fermi energy is then calculated to be 11.65 eV for Al and 3.24 eV for Na. For the model potential, we use the Ashcroft pseudopotential

$$v_{\text{ps}}(q) = -\frac{Z e^2}{\varepsilon_0 q^2} \cos(q r_c), \quad (11)$$

where r_c is the cutoff radius, which is set to be 0.5911 Å for Al and 0.8784 Å for Na [14]. For the correction $G(q)$ for exchange and correlation energies, we use the Hubbard-type function

$$G(q) = \frac{a q^2}{q^2 + b}, \quad (12)$$

where the parameters of a and b are determined from an analytical formula given in Ref. [15]. We have confirmed that the same conclusion (phonon hardening and softening with T_e) holds when $G(q)$ is set to be zero. We have also performed other bcc-structured crystals (Li, K, Rb, and Cs) and confirmed that the trend of their results is similar to that of Na shown below.

A. fcc-structured Al

Figure 1(a) shows the phonon dispersion relations of Al for $k_{\text{B}} T_e = 0.025, 2.0,$ and 4.0 eV. A significant increase in the phonon energies is observed at $k_{\text{B}} T_e = 4.0$ eV, which is consistent with the DFT results in Ref. [9, 10]. To understand the phonon hardening driven by an electronic excitation, we show T_e -dependence of A_p and B_p ($p = 1, 2, 3,$ and 4) in Fig. 1(b) and 1(c), respectively. The magnitude of B_1 starts to increase from $T_e \simeq 2$ eV, while that of B_p for $p \geq 2$ converges to zero, and A_1 decreases negatively. These changes are caused by the T_e -dependence of $V_{\text{tot}}(R)$ in Eq. (1), shown in Fig. 1(d). When $k_{\text{B}} T_e = 0.025$ eV, $V_{\text{tot}}(R)$ shows a Friedel oscillation that originates from the presence of the Fermi surface. As T_e increases, the oscillating amplitude becomes weak and thus the value of V_{tot} for $R/a_{\text{lat}} > 1$ becomes negligibly small, which lead to a significant decrease in B_p for $p \geq 2$. In addition, V_{tot} becomes more repulsive at $p = 1$ sites since $v_{\text{d}} \gg |v_{\text{ind}}|$. This also leads to an increase in $|A_1|$ and B_1 that are defined as Eqs. (9) and (10), respectively.

As is clear from Figs. 1(b) and 1(c), the lattice dynamics up to $k_{\text{B}} T_e = 4.0$ eV is almost regulated by B_1 only because $B_1 \gg |B_p|$ ($p = 2, 3,$ and 4) and $B_1 \gg |A_p|$. A simple analysis, where the contribution from A_p and B_p with $p \geq 2$ is ignored, enables us to understand the phonon hardening phenomena observed above. For example, we focus on the phonon frequency at the X point, at which the phonon frequencies are given by

$$\omega_{1,2} = \sqrt{\frac{8A_1 + 2B_1}{M_{\text{ion}}}}, \quad \omega_3 = \sqrt{\frac{8A_1 + 4B_1}{M_{\text{ion}}}}, \quad (13)$$

where ω_1 and ω_2 are the doubly degenerate TA phonon frequencies and ω_3 is the LA phonon frequency. From

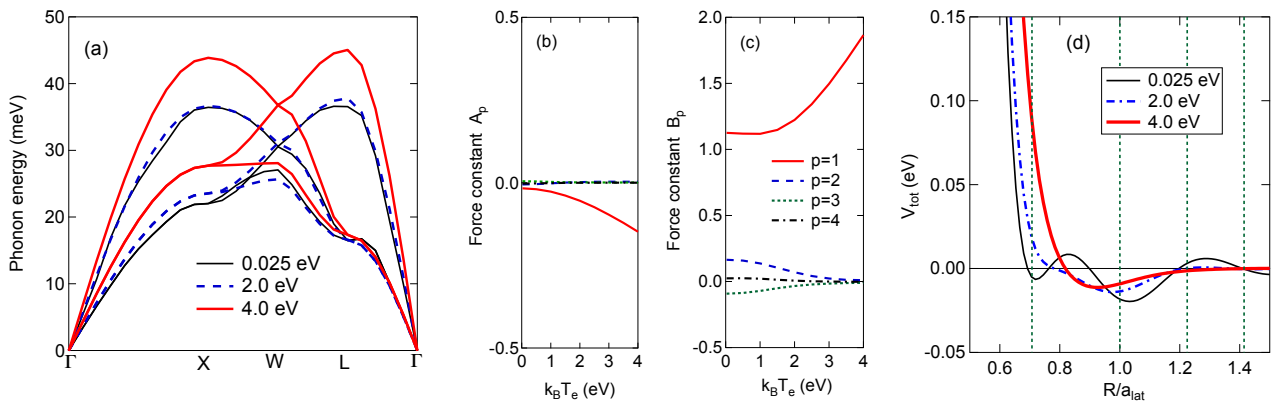


FIG. 1: (a) The phonon dispersion relations of fcc-structured Al along symmetry lines for $k_B T_e = 0.025$ (black), 2.0 (blue), and 4.0 (red) eV. T_e -dependence of the force constants (b) A_p and (c) B_p in units of $\text{eV}/\text{\AA}^2$. (d) The total potential V_{tot} defined as Eq. (1). The vertical dotted lines indicate the interatomic distance up to $p = 4$.

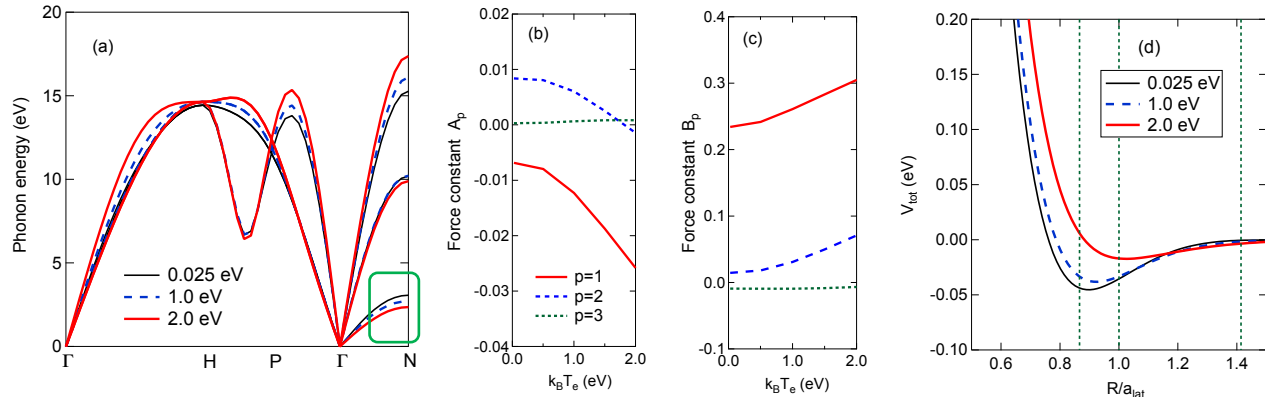


FIG. 2: Same as Fig. 1 but for Na. The phonon dispersion relations and V_{tot} are calculated for $k_B T_e = 0.025$, 1.0, and 2.0 eV. The lower frequency phonon at the N point decreases with T_e enclosed by a rounded rectangle. The interatomic distance is indicated up to $p = 3$.

Eq. (13), it is obvious that the increase in the phonon energy in Fig. 1(a) is directly related to the increase in B_1 .

B. bcc-structured Na

We next investigate the phonon properties of Na. Figures 2(a), 2(b) and 2(c), and 2(d) show the phonon dispersion relations (for $k_B T_e = 0.025$, 1.0, and 2.0 eV), A_p and B_p ($p = 1, 2$, and 3), and $V_{\text{tot}}(R)$, respectively. As shown in Fig. 2(a), the phonon energy increases slightly for higher frequency region, while the lowest phonon frequency at the N point decreases with T_e . Similar softening behavior and an imaginary frequency at the N point have been reported in Ref. [9, 10]. For lower T_e the lattice dynamics is almost regulated by B_1 again. However, the changes in A_1 , A_2 , and B_2 in response to T_e cannot be negligible. This is because the profile of V_{tot} is different from that in Al (Fig. 1(d)): The Friedel oscillation is not

clearly observed, since the value of k_F of Na is smaller than that of Al.

To understand the phonon softening at the N point, we derive analytical expressions for the phonon frequency. From Eq. (8), the frequencies at the N point are written as

$$\omega_1 = \sqrt{\frac{4(A_1 + A_2) + 2B_2}{M_{\text{ion}}}}, \quad (14)$$

$$\omega_2 = \sqrt{\frac{4(A_1 + A_2) + \frac{4}{3}B_1}{M_{\text{ion}}}}, \quad (15)$$

$$\omega_3 = \sqrt{\frac{4(A_1 + A_2) + \frac{8}{3}B_1 + 2B_2}{M_{\text{ion}}}}, \quad (16)$$

where A_p and B_p up to $p = 2$ are considered because the use of two parameters $A_1 (< 0)$ and B_1 only is not enough to obtain a dynamically stable structure at $T_e = 0$ K. We emphasize that the expression for the lowest frequency ω_1 in Eq. (14) does not include the largest force constant B_1 ;

The magnitude of ω_1 is determined by a delicate balance between A_1 , A_2 , and B_2 . Although B_2 increases with T_e , the amount of the increase is completely cancelled out by the decrease in A_1 and A_2 . The latter contributions are large enough to cause ω_1 to decrease with T_e .

The polarization vectors \mathbf{e}_1 , \mathbf{e}_2 , and \mathbf{e}_3 corresponding to ω_1 , ω_2 , and ω_3 in Eqs. (14)-(16), respectively, are written as

$$\mathbf{e}_1 = \frac{1}{\sqrt{2}} \begin{pmatrix} 0 \\ 1 \\ -1 \end{pmatrix}, \quad \mathbf{e}_2 = \begin{pmatrix} 1 \\ 0 \\ 0 \end{pmatrix}, \quad \mathbf{e}_3 = \frac{1}{\sqrt{2}} \begin{pmatrix} 0 \\ 1 \\ 1 \end{pmatrix}. \quad (17)$$

The vectors \mathbf{e}_i ($i = 1$ and 2) and \mathbf{e}_3 are perpendicular to and parallel to the N point wavevector $\mathbf{q} = (0, 1/2, 1/2)$ in units of $2\pi/a_{\text{lat}}$, respectively, which will be helpful to identify the soft mode experimentally.

It should be noted that also for simple cubic structured lattices B_1 is not entered into the expression of the phonon frequencies at points X and M, implying an appearance of the phonon softening with T_e . We thus speculate that the larger the NN coordination number Z_C , the stronger the bond strength against the electron excitation. In fact, it has been shown that an electronic excitation can lead to a phonon softening in Bi with $Z_C = 6$ [9, 16] and Si with $Z_C = 4$ [2, 9], while it leads to a phonon hardening in hexagonal closed-packed structure of Mg with $Z_C = 12$ [9].

IV. SUMMARY

We have studied the effect of the electron temperature on the phonon dispersion relations for fcc- and bcc-structured metals within a model pseudopotential approach. The phonon hardening and softening in simple metals are discussed in terms of the force constants and the adiabatic potential as a function of the electron temperature. The phonon hardening originates from a significant increase in the force constant for the first NN sites, while the phonon softening at the N point in bcc-structured metals originates from a delicate balance between force constants for the first and second NN sites.

The formulation of the present work can be extended to metals with d -electrons in a sense of the valence Z change as discussed in the study of warm-dense gold [17], while parametrizing the relationship between Z and T_e is necessary.

Appendix A: Effective ion-ion interaction

We outline the derivation of the ion-electron-ion interaction potential [12, 18] for the case of finite T_e by considering the effect of the electron-ion interaction to the total electron energy of the free-electron system.

The Schrödinger equation for the free-electron in a volume Ω is given by

$$H_0|\mathbf{k}\rangle = \varepsilon(\mathbf{k})|\mathbf{k}\rangle, \quad (A1)$$

where $\varepsilon(\mathbf{k}) = \hbar^2 k^2 / (2m)$ is the free-electron energy and $|\mathbf{k}\rangle = e^{i\mathbf{k}\cdot\mathbf{r}} / \sqrt{\Omega}$ is the electron eigenstate. \hbar is the Planck constant, m is the bare electron mass m , and \mathbf{k} is the wavevector. The Schrödinger equation for the electron in a crystal with the number of the unit cell N_c is given as

$$(H_0 + W)|\Psi\rangle = E|\Psi\rangle, \quad (A2)$$

where W is a weak periodic potential, to which the electron-electron (e-e) interaction is also included, and written as

$$W(\mathbf{r}) = \sum_j w(\mathbf{r} - \mathbf{R}_j) \quad (A3)$$

with $w(\mathbf{r} - \mathbf{R}_j)$ being the potential energy of the lattice sites \mathbf{R}_j . Within the perturbation theory, the electron wavefunction is written as

$$|\Psi\rangle = |\mathbf{k}\rangle + \sum_{\mathbf{q} \neq 0} \frac{\langle \mathbf{k} + \mathbf{q} | W | \mathbf{k} \rangle}{\varepsilon(\mathbf{k}) - \varepsilon(\mathbf{k} + \mathbf{q})} |\mathbf{k} + \mathbf{q}\rangle, \quad (A4)$$

while the electron eigenenergy is written as

$$E(\mathbf{k}) = \varepsilon(\mathbf{k}) + \langle \mathbf{k} | W | \mathbf{k} \rangle + \sum_{\mathbf{q} \neq 0} \frac{\langle \mathbf{k} + \mathbf{q} | W | \mathbf{k} \rangle \langle \mathbf{k} | W | \mathbf{k} + \mathbf{q} \rangle}{\varepsilon(\mathbf{k}) - \varepsilon(\mathbf{k} + \mathbf{q})}. \quad (A5)$$

The total energy per a unit cell is then given as

$$E_{\text{tot}} = \frac{2}{N_c} \sum_{\mathbf{k}} f(\mathbf{k}; T_e) E(\mathbf{k}) + E_{\text{dc}}, \quad (A6)$$

where $f(\mathbf{k}; T_e)$ is the Fermi-Dirac distribution function for the energy $E(\mathbf{k})$ and the temperature T_e , which is introduced in this work to account for the electron excitation. The prefactor 2 in the first term in Eq. (A6) comes from spin degeneracy. The second term E_{dc} accounts for the double-counting of the e-e interaction energy. As usual, we decompose E_{tot} into

$$E_{\text{tot}} = E_{\text{free}} + E_{\text{bs}}, \quad (A7)$$

where E_{free} is the free-electron energy that is independent of the ion position, while E_{bs} is the bandstructure energy that depends on the geometrical configuration of the ions. E_{bs} comes from both the last term of Eq. (A5) and E_{dc} , and can be expressed as

$$E_{\text{bs}} = \sum_{\mathbf{q} \neq 0} S^*(\mathbf{q}) S(\mathbf{q}) F(\mathbf{q}) \quad (A8)$$

with the structure factor

$$S(\mathbf{q}) = \frac{1}{N_c} \sum_j e^{-i\mathbf{k}\cdot\mathbf{R}_j} \quad (A9)$$

and the energy-wavenumber characteristic $F(\mathbf{q})$. By using Eq. (A9), one obtains

$$\begin{aligned} E_{\text{bs}} &= \frac{1}{N_c^2} \sum_{\mathbf{q} \neq 0} \sum_i \sum_j e^{i\mathbf{q} \cdot (\mathbf{R}_i - \mathbf{R}_j)} F(\mathbf{q}) \\ &= \frac{1}{2N_c} \sum_{i \neq j} v_{\text{ind}}(|\mathbf{R}_i - \mathbf{R}_j|) + \frac{1}{N_c} \sum_{\mathbf{q} \neq 0} F(\mathbf{q}), \end{aligned} \quad (\text{A10})$$

where $v_{\text{ind}}(|\mathbf{R}_i - \mathbf{R}_j|)$ is the indirect interaction potential between ions at \mathbf{R}_i and \mathbf{R}_j and expressed as

$$\begin{aligned} v_{\text{ind}}(|\mathbf{R}|) &= \frac{2}{N_c} \sum_{\mathbf{q} \neq 0} e^{i\mathbf{q} \cdot (\mathbf{R}_i - \mathbf{R}_j)} F(\mathbf{q}) \\ &= \frac{\Omega_a}{\pi^2} \int_0^\infty dq q^2 \frac{\sin(qR)}{qR} F(q) \end{aligned} \quad (\text{A11})$$

with $\Omega_a = \Omega/N_c$. We assumed that F depends on the magnitude of \mathbf{q} only. When the contributions from the Hartree, exchange, and correlation interactions are included to W , $F(q)$ can be written as [18]

$$F(q) = -\frac{\epsilon_0 q^2}{2e^2 \Omega_a} \frac{\chi(q, T_e) v_{\text{ps}}^2(q)}{1 + [1 - G(q)] \chi(q, T_e)}. \quad (\text{A12})$$

By substituting Eq. (A12) into Eq. (A11), we obtain the expressions in Eqs. (3) and (4).

-
- [1] Z. Lin, L. V. Zhigilei, and V. Celli, Electron-phonon coupling and electron heat capacity of metals under conditions of strong electron-phonon nonequilibrium, *Phys. Rev. B* **77**, 075133 (2008).
- [2] V. Recoules, J. Cl  rouin, G. Z  rah, P. M. Anglade, and S. Mazevet, Effect of Intense Laser Irradiation on the Lattice Stability of Semiconductors and Metals, *Phys. Rev. Lett.* **96**, 055503 (2006).
- [3] R. Ernstorfer, M. Harb, C. T. Hebeisen, G. Sciaini, T. Dartigalongue, R. J. D. Miller, The Formation of Warm Dense Matter: Experimental Evidence for Electronic Bond Hardening in Gold, *Science* **323**, 1033 (2009).
- [4] P. M. Leguay, A. L  vy, B. Chimier, F. Deneuville, D. Descamps, C. Fourment, C. Goyon, S. Hulin, S. Petit, O. Peyrusse, J. J. Santos, P. Combis, B. Holst, V. Recoules, P. Renaudin, L. Videau, and F. Dorchies, Ultrafast Short-Range Disorder of Femtosecond-Laser-Heated Warm Dense Aluminum, *Phys. Rev. Lett.* **111**, 245004 (2013).
- [5] B. I. Cho, T. Ogitsu, K. Engelhorn, A. A. Correa, Y. Ping, J. W. Lee, L. J. Bae, D. Prendergast, R. W. Falcone, and P. A. Heimann, Measurement of Electron-Ion Relaxation in Warm Dense Copper, *Sci. Rep.* **6**, 18843 (2016).
- [6] F. Dorchies, V. Recoules, J. Bouchet, C. Fourment, P. M. Leguay, B. I. Cho, K. Engelhorn, M. Nakatsutsumi, C. Ozkan, T. Tschentscher, M. Harmand, S. Toleikis, M. St  rmer, E. Galtier, H. J. Lee, B. Nagler, P. A. Heimann, and J. Gaudin, Time evolution of electron structure in femtosecond heated warm dense molybdenum, *Phys. Rev. B* **92**, 144201 (2015).
- [7] S. Groth, T. Dornheim, T. Sjostrom, F. D. Malone, W. M. C. Foulkes, and M. Bonitz, Ab initio Exchange-Correlation Free Energy of the Uniform Electron Gas at Warm Dense Matter Conditions, *Phys. Rev. Lett.* **119**, 135001 (2017).
- [8] D. V. Minakov and P. R. Levashov, Melting curves of metals with excited electrons in the quasiharmonic approximation, *Phys. Rev. B* **92**, 224102 (2015).
- [9] G. Q. Yan, X. L. Cheng, H. Zhang, Z. Y. Zhu, and D. H. Ren, Different effects of electronic excitation on metals and semiconductors, *Phys. Rev. B* **93**, 214302 (2016).
- [10] L. Harbour, M. W. C. Dharma-wardana, D. D. Klug, and L. J. Lewis, Equation of state, phonons, and lattice stability of ultrafast warm dense matter, *Phys. Rev. E* **95**, 043201 (2017).
- [11] F. Bottin and G. Z  rah, Formation enthalpies of monovacancies in aluminum and gold under the condition of intense laser irradiation, *Phys. Rev. B* **75**, 174114 (2007).
- [12] W. M. Hartmann and T. O. Milbrodt, Model-Potential Calculations of Phonon Energies in Aluminum, *Phys. Rev. B* **3**, 4133 (1971).
- [13] N.W. Ashcroft, N. D. Mermin, and D. Wei, *Solid State Physics*, revised edition, (Cengage, Boston, 2016).
- [14] N. W. Ashcroft, *Phys. Lett.* **23**, 48 (1966).
- [15] S. Ichimaru and K. Utsumi, Analytic expression for the dielectric screening function of strongly coupled electron liquids at metallic and lower densities, *Phys. Rev. B* **24**, 7385 (1981).
- [16]   . D. Murray, S. Fahy, D. Prendergast, T. Ogitsu, D. M. Fritz, and D. A. Reis, Phonon dispersion relations and softening in photoexcited bismuth from first principles, *Phys. Rev. B* **75**, 184301 (2007).
- [17] C. Fourment, F. Deneuville, D. Descamps, F. Dorchies, S. Petit, O. Peyrusse, B. Holst, and V. Recoules, Experimental determination of temperature-dependent electron-electron collision frequency in isochorically heated warm dense gold, *Phys. Rev. B* **89**, 161110(R) (2014).
- [18] G. Grimvall, *The Electron-Phonon Interaction in Metals*, (North-Holland, Amsterdam, 1981).